IRISH CHEMICAL NEWS

Research Article

‘Rusty’ metal electrodes : redox chemistry and electrochemical water splitting catalysis

Michael E G Lyons*, Richard L. Doyle, Ian Godwin, Anja Cakara, Patrick O’Brien, Maria O’Brien and Lisa Russell

Trinity Electrochemical Energy Conversion & Electrocatalysis (TEECE) Group, School of Chemistry & CRANN, Trinity College Dublin 2, Ireland
E-mail: melyons@tcd.ie

Introduction

The oxygen evolution reaction (OER) is the anodic reaction that accompanies, in aqueous electrolytes, commercially important cathodic processes such as metal electrowinning[1] and hydrogen production via alkaline water electrolysis[2].The latter has been proposed as an environmentally inoffensive route to the production of large volumes of pure hydrogen gas required by a possible hydrogen economy[3] (see figure 1). For the latter process the anodic overpotential is the major factor in limiting operational efficiency[4]. Over the past 30 years, considerable research effort has been devoted to the design, synthesis and characterization of OER anode materials, with the aim of achieving useful rates of active oxygen evolution at the lowest possible over-potential, in order to optimize the overall electrolysis process. Currently, the optimal OER anode materials are RuO_2 and IrO_2 since these oxides exhibit the lowest overpotentials for the OER at practical current densities[5]. However the high cost of these materials and their poor long term stability in alkaline water electrolysis cells renders their widespread commercial utilization both uneconomical and impractical[6], however they have been shown to be quite stable in polymer electrolyte membrane (PEM) cells. In light of these limitations, the oxides of the first row transition metals offer a compromise solution. Iron and nickel electrodes are interesting candidates. Although they possess inferior electrocatalytic activity for the OER, their relatively low cost and long term corrosion resistance in alkaline solution make them attractive OER anode materials[7].

The mechanism of the OER at first row transition metal oxide surfaces remains controversial and the important question of whether a possible common mechanism can be formulated, which would facilitate a theory of electrocatalysis for oxygen evolution is currently unresolved. It is our opinion that a systematic and consistent study of the OER at the oxidized surfaces of electrodes of adjacent first row transition metals should prove useful in eluciding whether a common reaction mechanism prevails.

In the present paper we report on recent studies performed within the TEECE Group on examining the mechanism of oxygen evolution at iron and nickel oxyhydroxide film coated electrodes in aqueous base. We propose a mechanism for the OER reaction which specifically takes into account the nature of the electrochemically generated hydrous metal oxide film present on the metal surface during active oxygen evolution.

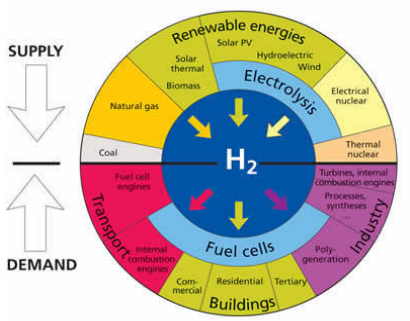

Figure 1. Electrochemical Ying/Yang. Schematic representation of hydrogen used as energy vector. Hydrogen can be generated via water electrolysis, and consumed as a fuel in a fuel cell for electricity generation.

Electrochemically induced generation of metal oxy-hydroxide thin films on electrode surfaces

We classify metal oxides into two groups[8]. The first are termed compact, anhydrous oxides such as rutile, perovskite and spinel in which oxygen is present only as a bridging species between two metal cations and ideal crystals constitute tightly packed giant molecules. The second class are dispersed, hydrous oxides where oxygen is present not just as a bridging species between metal ions, but also as O^-, OH and OH_2 species in co-ordinated terminal group form. In many cases, the latter materials when in contact with aqueous media, contain considerable quantities of loosely bound and trapped water plus, on occasion electrolyte species. It should be noted[8] that with microdispersed species the boundary between the solid and aqueous phase may be nebulous as the two phases virtually intermingle. This will be important when a simple physical model is developed to aid the understanding of the redox switching behaviour observed in thin films of the latter materials[9].

Furthermore, while compact oxides are usually prepared by thermal techniques such as for example decomposition of an inorganic salt precursor in air at elevated temperatures (RuO_2 and IrO_2 are typically formed at 450ºC), the dispersed oxides are almost invariably prepared in an aqueous environment using base precipitation of electrochemical techniques. We focus attention on the latter preparation methods here. In the latter methodology,

the potential applied to the parent metal (or indeed to an inert metal support if film formation is accomplished via electro-precipitation from a metal salt solution) is cycled (or pulsed) in a repetitive manner between suitable upper and lower limits in an aqueous solution of appropriate pH. It is important to emphasise here that the oxide materials deposited via such procedures are deposited in the kinetically most accessible, rather than the thermodynamically most stable form. As a consequence the redox behaviour of the film will exhibit time varying effects. The deposited films are often amorphous or only poorly crystalline and will be prone to rearrangement in a manner that is directly influenced by factors such as temperature, pH and ionic strength. Microdispersion is usually due to the presence of strand, layer, tunnel or cage structures which facilitate not just small ions, but also in many cases solvent molecules to permeate the oxide or oxy-hydroxide phase.

One of the most versatile and convenient techniques used to generate hydrous metal oxy-hydroxide modified electrodes in a form suitable for the real time determination of their redox switching and electrocatalytic behaviour is that of repetitive potential multicycling (RPM). Here the electrode of the parent metal is cycled repetitively between suitable lower and upper limits in an aqueous alkaline or indeed acid solution. The RPM technique has been used to form oxide layers on many metals such as Fe, Ni, Co, Rh, Ir, Pt, Pd, Mn, and Cu. The type of potential perturbation used for oxide growth –sinusoidal, square or triangular wave- apparently makes little difference. Indeed the triangular wave is the most convenient, as changes in the current vs potential response profile (termed the cyclic voltammogram) can be employed during the oxide deposition reaction to monitor changes in redox behaviour associated with the latter as illustrated below in fig.2 for the growth of hydrous oxy-hydroxide films on Fe electrodes in aqueous 0.5 M NaOH.

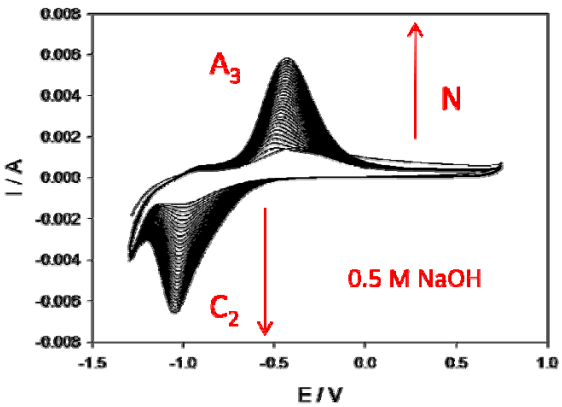

Figure 2 Growth of hydrous iron oxy-hydroxide thin film on Fe support electrode monitored via analysis of the real time voltammogram in 0.5 M NaOH. Potential swept between – 1.30 V and 0.75 V (vs Hg/HgO) at a sweep rate of 400 mV/s.

The growth of the hydrous oxide film on the Fe electrode can be readily monitored by following the development of the set of redox peaks labelled A_3,C_2 as a function either of the time or the number of potential cycles N. The variation of the integrated redox charge capacity Q (the latter is directly related to the hydrous oxide layer thickness L) as a function of number of cycles N is outlined in fig.3 below.

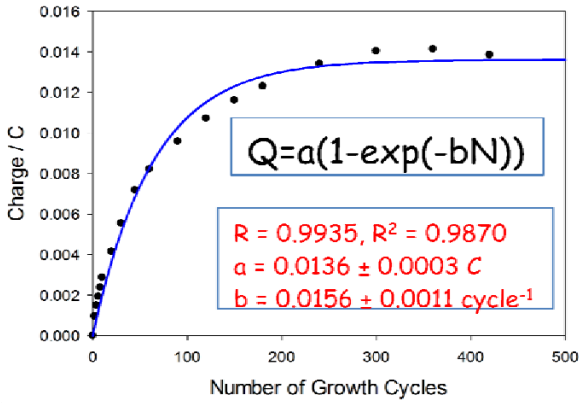

Figure 3 Growth of hydrous iron oxy-hydroxide thin film on Fe support electrode monitored via analysis of the real time voltammogram in 0.5 M NaOH. Potential swept between – 1.30 V and 0.75 V (vs Hg/HgO) at a sweep rate of 400 mV/s.

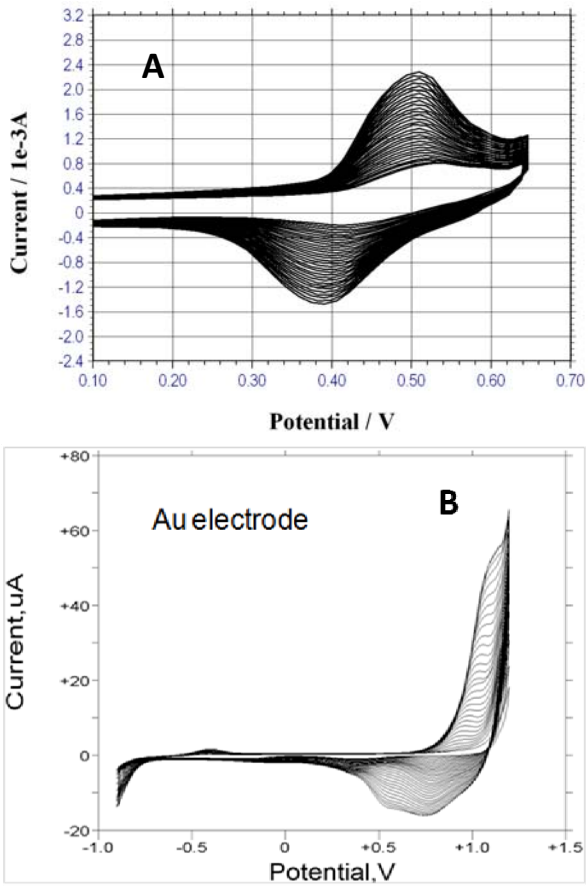

Figure 4 (a) Growth of nickel oxy-hydroxide thin film on Ni metal support electrode in 1.0 M NaOH. Growth potential limits: - 1.45 V to 0.65 V (vs Hg/HgO), sweep rate 150 mV/s, N = 30 cycles. (b) Growth of nickel oxy-hydroxide thin film on Au support electrode monitored via analysis of the real time voltammogram in $_{Ni}^{2+}$ containing aqueous acetate buffer solution, pH 7.6. The potential was cycled from – 900 mV to + 1200 mV (the latter potentials were measured with respect to a SCE in the acetate buffer medium) at a potential sweep rate of 50 mV/s.

In fig.3 the data can be fit adequately to the latter expression

$$Q = a\{1 - \exp[-bN]\} \quad (1)$$

This expression implies that as N → ∞, Q → a which is a constant limiting value. Furthermore the rate of increase of oxide growth dQ/dN decreases in a regular manner with increasing number of cycles N.

As illustrated in fig.4 the RPM technique can also be applied to deposit a hydrous nickel oxy-hydroxide thin film on either a Ni metal electrode in aqueous base or on a Au support electrode from a buffer solution containing Ni^{2+} ion (Pt and GC electrodes are also good supports). The developing redox behaviour of the immobilized nickel ion sites in the film can be readily monitored in real time by examination of the developing voltammograms.

The mechanism of hydrous oxide growth via RPM is now reasonably well understood, at least at a qualitative level[10,11]. It may be assumed that the initial oxidation process involves the formation of reversibly adsorbed OH and O moieties on the metal surface. With increasing degree of surface coverage adsorption assumes a more irreversible character accompanied by the formation, via a place exchange mechanism, of a thin, largely anhydrous, compact passivating phase oxide layer. Under conventional steady state anodization conditions where a steady oxidizing potential is applied to the metal surface such layers are of limited thickness as the activation energy for atom or ion migration in the compact film is usually quite large.

Even though it is directly produced in the initial electrochemical oxidation process, the anhydrous film is probably not the most stable metal oxidation product in the aqueous medium, but it may be regarded as an intermediate or metastable product in the formation of the hydrous oxide layer. In the anhydrous film ions are held in a rigid manner in an extended network of polar covalent bonds which drastically reduce ion transport through (and consequently extension of) the surface layer. The next stage of the film thickening reaction is the hydration process, and is generally very slow. This is because as in phase transformation reactions, it involves rupture of primary coordination metal-oxygen bonds. We have established in previous studies that the extent of hydrous oxide growth depends on the value chosen for the upper and lower limit of the potential sweep. As well as on the cycling frequency adopted and the solution temperature and pH employed during the RPM procedure.

The chemistry involved in film formation can be complex. For example referring to the data outlined in fig.4 for nickel oxy-hydroxide film deposition in aqueous buffer We note that the electro-deposition process may proceed as follows:

$$Ni^{2+}(aq) + 2\,OH^- \rightarrow Ni(OH)_2 \quad (2)$$

The following process may also occur as the applied potential becomes more anodic:

$$OH^- \rightarrow OH_{ads} + e^- \quad (3)$$

$$Ni^{2+}(aq) + H_2O + OH_{ads} \rightarrow NiOOH + 2\,H^+(aq) \quad (4)$$

The following process may also occur in the solution:

$$Ac^- + H_2O \rightarrow HAc + OH^- \quad (5)$$

$$Ni^{2+}(aq) + OH^- \rightarrow NiOH^+(aq) \quad (6)$$

$$NiOH^+ + OH_{ads} \rightarrow NiOOH + 2\,H^+ \quad (7)$$

Hence we infer that both $Ni(OH)_2$ and NiOOH may well be formed during the course of the potential sweep perturbation. Unravelling the details of the redox chemistry which underlie the oxide film deposition can indeed be complex, and one needs to apply a combination of gravimetric and spectroscopic techniques to fully elucidate the mechanism[12].

Hence under conditions of thick film growth produced via potential cycling the interfacial region may be represented by the following: $M/MO_x/(MO)_a(OH)_b(OH_2)_c$/aqueous phase, as outlined in fig.5 below. This is the Duplex Layer Model of the oxide/solution interface region first proposed by Burke et al[13] some time ago.

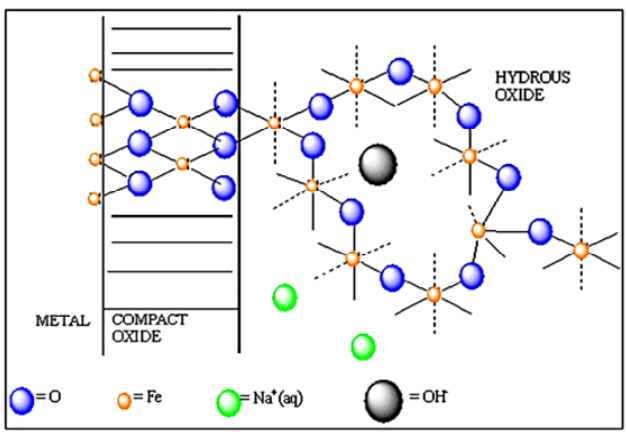

Figure 5 Schematic representation of Duplex Layer Model of oxide/solution interface.

The inner compact oxide layer is usually extremely thin, typically 1-5 monolayers in extent. The outer hydrous layer is regarded as extensively hydrated with both bound and trapped water present, as well as anions and cations. Hence we conclude that the hydrous oxide film can be regarded as an extended surface bonded polynuclear species. Metal cations in the polymer network are held together by a sequence of oxy and hydroxyl bridges. In short we can regard the microdispersed hydrous oxide layer as an open porous mesh of interconnected octahedrally coordinated surfaquo metal oxy groups. Burke and O'Sullivan[13] have suggested that the compact film component of the duplex oxide is highly conducting, with little potential drop across the inner layer. The major potential drop is assumed to occur at the outer surface of the compact film where the hydrous oxide is located (fig.5). As noted in fig.2 and indeed in fig.3 the growth of the hydrous oxide layer on cycling is not accompanied by any notable increase in charge associated with the double layer region. This suggests that the electrode area remains constant despite the formation of a thick, quite visible porous oxide film.

A possible explanation of the observed constancy of the double layer currents exhibited in fig.2 and fig.3 is that the compact oxide/hydrous oxide interface (the region of maximum potential drop) is the only region where a faradaic electron transfer reaction occurs. The material in the hydrous layer is so dispersed that it does not behave as a separate bulk phase distinct from the electrolyte solution. Hence the hydrous oxide strands and solution do not form separate phases. The oxide might well not exhibit such bulk characteristics as a distinct three dimensional electronic band structure or a well defined oxide/solution phase boundary. This concept is borne out by ellipsometric measurements where the apparent refractive index exhibits a very low value and the film density is low.

The marked dependence of oxide growth rate on the lower limit of the potential sweep is indicative of the essential role that partial reduction of the anhydrous oxide plays in the production of a thick deposit. Partial reduction of the compact oxide layer apparently facilitates rearrangement of oxy-cation species at the metal surface, leaving it in a somewhat disrupted state. It has been established for a number of metals that the anhydrous film is reduced much more readily than the hydrated film. The greater stability of the latter is probably due to reasons such as (i) lower repulsion between cations owing to greater separation, (ii) decreased net charge arising from hydroxyl ion coordination by cations present and (iii) polymer formation. On subsequent re-oxidation of the partially reduced metal surface the compact layer is restord but the outer region of the compact film is present in a more dispersed form. On further reduction the latter material becomes incorporated into the outer hydrated layer. It is not clear whether this rearrangement process involves the detachment of oxycations, i.e. a dissolution/re-precipitation mechanism, or a certain weakening, with only a partial detachment of oxy-cation binding in the compact oxide layer. In the latter case the partially reduced cations are assumed to be displaced from normal lattice sites, and, as such, are more susceptible to oxidation in the subsequent anodic sweep during which they complete their oxygen coordination shell of six oxygen atoms to form a rather open polymeric inorganic bronze or zeolite type structure.

The upper limit of the potential sweep also has an important effect on the rate of oxide growth. The importance of this parameter lies in the fact that it extends oxygen penetration into the outer regions of the metal lattice, and may also help to generate a slight expansion and stress associated disruption of the metal/oxide interface. The upper potential limit may also facilitate uptake of a slight excess of oxygen by the oxide phase. A common observation in our studies is that there is an optimum value of upper limit. The fall of in oxide growth efficiency at more anodic values of applied potential may be associated with the increasing difficulty of reduction of the passivated surface film at lower potentials when the potential sweep is subject to reversal. Hence the optimum upper limit corresponds to a potential which represents the best compromise between two opposing effects. In short the compact layer must attain a reasonable thickness (hence the need for a relatively high anodic potential), but too high an upper limit results in a very un-reactive layer which does not reduce readily at the lower potential limit.

Hence for most metals, but especially for the noble metals such as Au, Pt, Ir and Rh, extension of oxide growth beyond the monolayer level under conventional galvanostatic or potentiostatic (constant current or potential) conditions is usually quite slow. This is obviously due to the presence of the initial compact oxide product layer which acts as a passivating diffusive barrier to further growth via ion migration (such compact oxides often exhibit parabolic growth kinetics). In contrast under potential cycling conditions the upper limit plays a significant role. There is probably a combination of thermodynamic and kinetic factors involved, but evidently the upper limit must be sufficiently anodic that compact oxide formation exceeds significantly the single monolayer level so that on subsequent reduction, a disturbed, highly disordered layer of metal atoms is prepared on the metal surface (see fig.5). Thus with Pt and Au, two metals where oxide monolayer behaviour is well defined[14], the optimum lower limit lies at a potential value at, or below, the value of the monolayer oxide reduction peak. On subsequent re-oxidation the disturbed layer of metal atoms is converted to hydrated or partially hydrated oxide – complete hydration under these circumstances may involve several redox cycles- with a fresh inner compact layer being regenerated at the metal surface on each anodic sweep. On repetitive potential cycling the porous outer layer increases in thickness at the expense of the underlying metal.

Finally the decrease in oxide growth rate with number of cycles, time (or equivalently with increasing film thickness expressed quantitatively via $dQ/dN = ab\exp[-bN]$, can be attributed to the increasing inhibition of water and hydroxide ion transfer to the inner region of the oxide layer, with increasing hydrous oxide thickness. We have observed that this effect is more marked with increasing base concentration. Evidently, increased hydroxide ion activity suppresses hydroxide ion dissociation and/or favours adsorption of this species. This will result in the inhibition of crystallization of the hydrous oxide layer, and the resulting more amorphous film will be more effective in excluding water from the inner region of the oxide film, thereby inhibiting growth of the microdisperse hydrous layer.

Redox switching in multilayer hydrous oxide films

We now describe the electrochemical properties of hydrous oxyhydroxide thin film modified electrodes which are formed via potential cycling in aqueous base. We focus particular attention on nickel oxy-hydroxide films in which the metal oxide is deposited electrochemically on either a Ni or Au support surface. The discussion will focus on the redox switching reaction within the hydrous oxide layer in which the oxymetal sites charge oxidation state via potential induced topotactic redox reactions involving electron transfer between adjacent metal ion sites along the polymeric oxide strand and charge compensating counter ion transport within the solution region between the oxide strands. We focus attention on the latter process since it defines many of the practical applications of the oxide electrode such as its capacity to store charge (useful in supercapacitor applications), to change colour when the oxidation state is changed

(electrochromic behaviour) and to serve as an effective pH and chemical sensor.

Typical cyclic voltammetric profiles recorded for multicycled (N = 30 cycles in both cases) Ni and Au electrodes modified with a nickel oxy-hydroxide film in contact with aqueous 1.0 M NaOH are outlined in fig.6. In fig .6(a) the oxide layer was grown on a Ni electrode in 1.0 M NaOH by cycling the potential between limits of – 1.45 V to 0.65 V (vs Hg/HgO) at a sweep rate of 150 mV/s. In fig.6(b) the oxide layer was deposited on an Au support surface from a deposition solution of 0.1 M $NiSO_4$, 0.1 M NaAc and 0.001 M NaOH between limits of – 0.90 to 1.20 V (vs SCE) at a sweep rate of 20 mV/s.

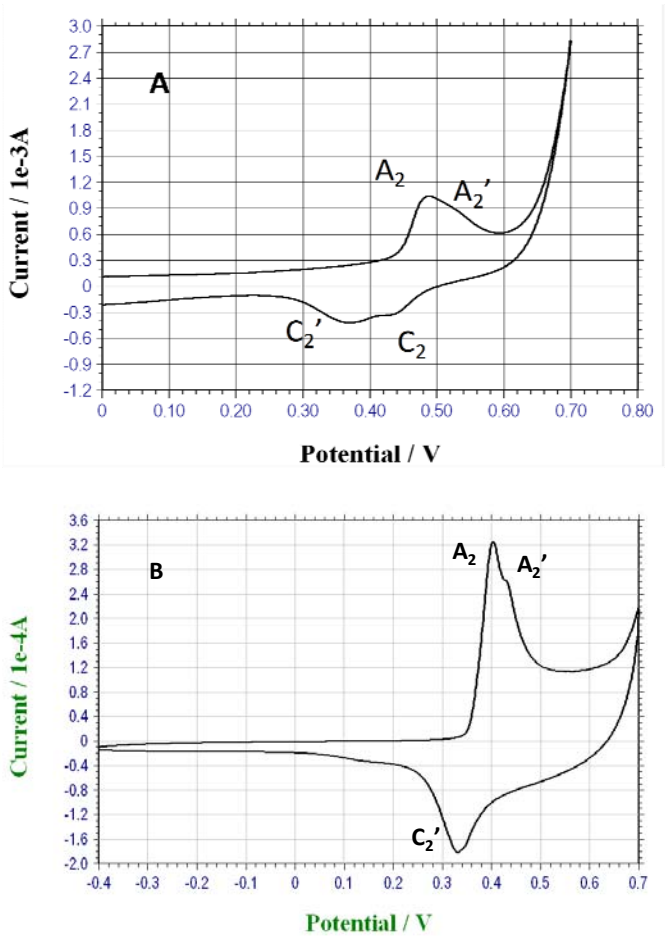

Figure 6 (a) Typical voltammetric response recorded for a hydrous nickel oxy-hydroxide thin film on Ni support electrode in 1.0 M NaOH. Sweep rate, 40 mV/s. Layer grown for N = 30 cycles. (b) Voltammetric response recorded for an electroprecipitated nickel oxyhydroxide modified Au electrode in 1.0 M NaOH. Sweep rate, 40 mV/s.

It is clear from fig. 6 that the voltammetric behaviour recorded for the nickel oxy-hydroxide thin films grown both on Ni and Au support electrodes is similar in that two sets of peaks may be observed in the potential region 0.30 – 0.60 V (vs Hg/HgO) prior to the onset of active water oxidation to generate molecular oxygen. These peaks correspond to redox reactions involving the transfer both of electrons and ions within the microdispersed oxide film. The interfacial redox chemistry of the multicycled nickel oxide electrode in aqueous alkaline solution can be readily understood in terms of the Bode scheme of squares[15] as presented in scheme 1 and fig.7 below.

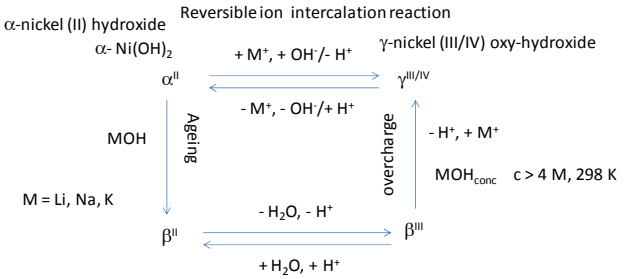

Scheme 1. Bode square scheme for redox switching in nickel oxy-hydroxide thin films .

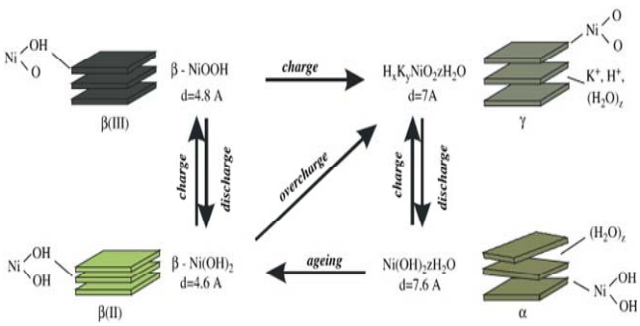

Figure 7. Structural representation of Bode square scheme.

The redox chemistry has been largely elucidated using electrogravimetric methods such as the Electrochemical Quartz Crystal microbalance which enables tiny mass changes which occur in the deposited thin film during redox switching to be monitored in real time[16]. Here the redox switching behaviour of electrochemically generated nickel oxide films was rationalized in terms of four phases as outlined in fig. 7. The discharged or reduced $Ni(OH)_2$ material can exist either as a largely anhydrous phase designated as β – $Ni(OH)_2$ (denoted β-Ni(II)) or as a hydrated phase denoted as α-$Ni(OH)_2$ (in short represented as α-Ni(II)). Oxidation of the β-Ni(II) material is envisaged to produce a phase referred to as β-NiOOH or β-Ni(III). In contrast oxidation of the α-Ni(II) material produces γ-Ni(III) or γ-NiOOH. Hence one expects two distinct redox transitions : α(II)/γ(III) which we label RT1 and β(II)/β(III) which is RT2. The corresponding redox peaks are designated A_2'/C_2' and A_2/C_2 respectively. A general representation of the RT1 and RT2 stoichiometry are outlined below.

$$\left[(1+x)\alpha - Ni(OH)_2 w_\alpha OH_2 \bullet (\delta_\alpha NO_3^-, \sigma_\alpha CO_3^{2-})\right] + y\left(Na^+ + OH^-\right) + (1+2x)OH^-$$

$$\left[\gamma - NiOOH.xNiO_2.w_\gamma OH_2 \bullet \left(\delta_\gamma NO_3^-, \sigma_\gamma CO_3^{2-}\right)\right] + \left(1+2x+w_\alpha - w_\gamma\right)OH_2 + (1+2x)e^-$$

$$\beta - Ni(OH)_2 \bullet w_\beta OH_2 + OH^- \rightleftharpoons \beta - NiOOH + (1 - w_\beta)OH_2 + e^-$$

We note that the redox potentials of RT1 is typically some 60-100 mV less positive than those of RT2. It can be noted from fig. 8 that upon ageing the α-$Ni(OH)_2$ can dehydrate and re-crystallize as β-$Ni(OH)_2$. This is especially prevalent in more concentrated alkali solution. In addition, overcharging β-NiOOH (which occurs at more elevated potentials) can convert it to γ-NiOOH. The non-stoichiometric nature of both the discharged and charged material is indicated by the average oxidation state of Ni in each phase as indicated in the structural representation of the various phases in fig. 7. It is important to note that while there is a general acceptance for the general features of the Bode scheme, one must understand that it is inappropriate to think about the formation of a compound or a phase with definite stoichiometry during the chemically complex $Ni(OH)_2$/NiOOH transformation. Instead the four phases mentioned in the Bode scheme should be considered as the limiting forms of the divalent and trivalent materials – the actual composition of the oxide at a given potential depending on a range of factors including its history, method of preparation, degree of hydration, defect concentration etc.

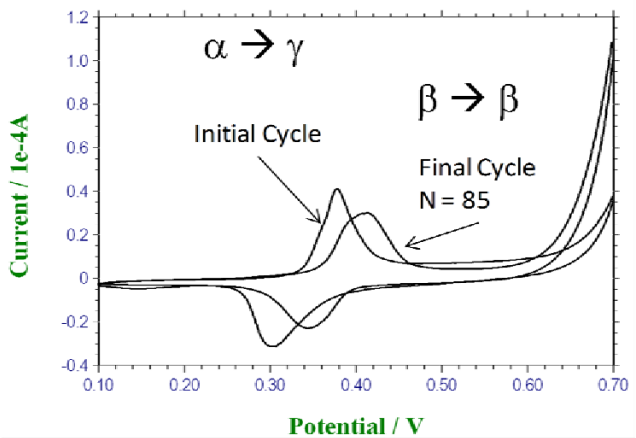

Figure 8. Typical voltammetric response recorded for an electroprecipitated nickel oxide film deposited on a polycrystalline gold substrate subjected to slow multicycling (sweep rate 10 mV/s) between 0.1 and 0.7 V (vs Hg/HgO) in 5.0 M NaOH. The initial and final response profiles are presented.

Burke and Lyons[17] and more lately, Lyons et al [18] have shown that, for an ideal oxide electrode system in aqueous solution at 25ºC, the potential decreases with increasing pH by ca. 59 mV/pH unit with respect to a pH independent reference electrode such as the NHE or the saturated calomel electrode (SCE). Such a potential-pH shift is referred to as a *Nernstian shift*, since it is predicted by the Nernst equation. Alternatively, if the reference electrode is pH dependent, such as the reversible hydrogen electrode (RHE) or the Hg/HgO electrode, no potential pH shift will be observed, since the potential of this type of electrode also alters by ca. 59 mV per unit change in pH at 25ºC. Furthermore, Burke and Lyons[17] have discussed super-Nernstian shifts that have been observed for various hydrous oxide systems – in these cases the potential/pH shift differs from the expected 0.059V/pH unit at 25°C. The mathematical treatment of this situation is beyond the scope of the present paper, but suffice to say, the phenomena have recently been qualitatively summarized[18]. Thus, a zero potential shift (with respect to a pH dependent reference electrode) implies that both the reactants and the product possess the same net charge. A positive potential shift with pH, is indicative of an oxidised state that is more positive than the reduced state, whereas the converse is true in the case of an observed negative potential/pH shift.

As previously shown[17,18] that the anhydrous A_2'/C'_2 peaks exhibit a regular Nernstian shift whereas the hydrous counterparts A_2/C_2 exhibit the characteristic of a hydrous or hyper-extended oxide i.e. *a super-nernstian potential-pH shift*, which typically has the value of $dE/dpH = -2.303(3RT/2F) = -0.088$V/pH unit at T = 298 K. Accordingly, by analogy with a scheme produced by Burke and Whelan[19] for redox switching of iridium oxide films, it has been proposed that the main redox switching reaction (corresponding to the peak set A_2/C_2) may be written as:

$$[Ni_2(OH)_6(OH_2)_3]_n^{2-} + 3nOH^- \rightarrow [Ni_2O_3(OH)_3(OH_2)_3]_n^{3-} + 3nH_2O + 2ne^- \quad (8)$$

corresponding to an Ni(II)/Ni(III) redox transition in a polymeric microdispersed hydrous oxide layer. This redox switching reaction is illustrated schematically in scheme 2.

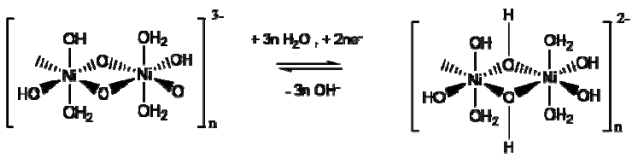

Scheme 2. Redox switching in hydrous nickel oxy-hydroxide matrix involving electron/ion exchange.

The redox switching reaction (associated with the A_2/C_2 voltammetric peaks) reflects the change in oxidation state of the film as a result of a potential perturbation. Redox centres immediately adjacent to the support electrode are directly affected by the electrode potential, whereas charge is further propagated along the oxy-nickel polymer strands in the hydrous layer via a sequence of electron self exchange reactions between neighbouring oxy-metal sites. This process is envisaged to be analogous to redox conduction exhibited by electroactive polymer films. In the simplest terms this electron "hopping" may be modelled in terms of a diffusional process, and so the charge percolation rate may be quantified in terms of a *charge transport diffusion coefficient*, D_{CT} or in terms of a diffusive frequency $\tau = D_{CT}/L^2$ where L denotes the thickness of the oxide film. . In the case of hydrous nickel oxide, the latter may reflect either the electron hopping rate or the diffusion of of OH^- (or equivalently H_3O^+) ions via a rapid Grotthuss type mechanism. The charge transport diffusion coefficient may be quantitatively estimated using cyclic voltammetry [20]. The important point to note is that

redox switching in the oxide involves electron and ion transport. The Ni(II)/Ni(III) redox transition occurs within a polymeric microdispersed oxide consisting of polymer strands comprising of interlinked octahedrally coordinated surfaquo groups. The assembly can be regarded as a dual rail electrical transmission line of the type presented in fig.9 for porous modified electrodes[21]. Hence the charge transport through the layer can be characterized in terms of characteristic resistances for electron and counter-ion motion along the oxide polymer strands and within the solution filled pores between the oxide strands. This type of conductivity characterization can be best accomplished using Electrochemical Impedance Spectroscopy[21]. The latter technique is very powerful and has been applied to mixed conducting systems in thin film form such as metal oxides and electronically conducting polymers[22].

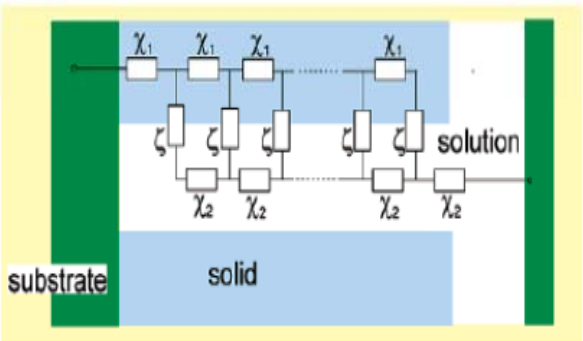

Figure 9 Dual rail transmission line model for porous thin film mixed electronic/ionic conductor. Note that χ_1 and χ_2 corresponds to the specific conductivity of the solid oxide phase and electrolyte solution respectively and ζ represents the specific polarization/charge transfer element at the solid/solution interface.

Multilayer hydrous oxide films as potential pH sensors

The fact that nickel oxy-hydroxide films exhibit a Super-Nernstian decrease in the peak potential associated with the Ni(II)/Ni(III) surface redox switching with increasing solution pH is significant for two reasons. The first signifier is that the oxy metal species must be anionic [17,18]. The second is that the oxide film may prove useful for pH detection. The variation is open circuit potential with solution pH for an electroprecipitated nickel oxy-hydroxide film on a gold substrate is presented schematically in figure 10. The open circuit potential was recorded for a range of time scales varying from 200 to 15,000 seconds. A good linear response of potential to changes in solution pH was recorded. The slope or super-Nernstian with $dE_{OC}/d\ pH = -0.080$ V/dec and $r^2 = 0.95$. The behaviour of the oxide pH sensor was examined by monitoring the response of the latter to the rapid changes in solution pH encountered during the course of a pH titration. The titration of 1M sulphuric acid H_2SO_4 with a strong base (50 mL 1 M NaOH) was monitored in real time using both a conventional glass electrode and the metal oxide modified electrode. The open circuit of the latter was determined as a function of volume of strong acid added to the reaction mixture.

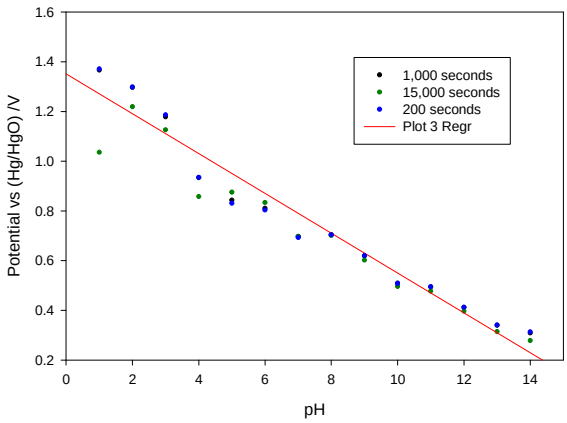

Figure 10 Variation of open circuit potential recorded at an electroprecipitated nickel oxyhydroxide modified gold electrode as a function of solution pH (the latter measured using a glass electrode).

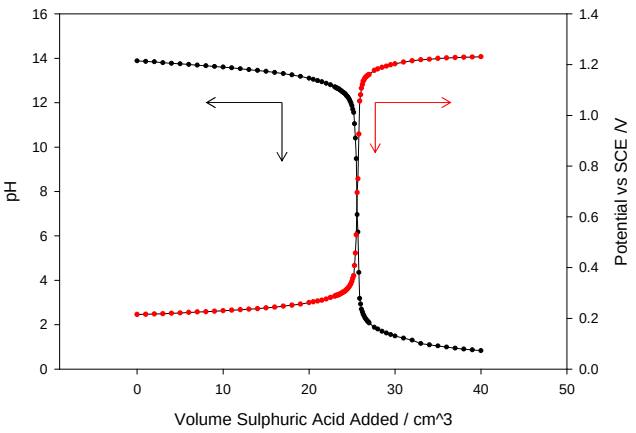

Figure 11 Variation of open circuit potential recorded at an electroprecipitated nickel oxyhydroxide modified gold electrode as a function of solution pH (the latter measured using a glass electrode) during the course of a strong acid/strong base titration.

It is indeed gratifying to note that the metal oxide wire electrode potential (measured with respect to a SCE reference electrode) monitors accurately the change in solution pH (measured using a commercial glass electrode system). The solid state pH sensor responds very rapidly to the rapid changes in pH recorded near the equivalence point. As the solution becomes more alkaline the open circuit potential of the oxide electrodes increases in a well defined manner. The metal oxide electrode accurately predicts the position of the equivalence point. Furthermore we have shown that an excellent correlation exists between the pH value calculated from the E_{OC} magnitude and that experimentally measured using a commercial glass electrode. Hence we conclude that electro-precipitated nickel oxyhydroxide thin film electrodes offer potential as novel pH sensors[23] .

The kinetics and mechanism of electrolytic water oxidation to generate molecular oxygen

The generation of molecular oxygen via electrolysis of water (OER) is a complex and energetically demanding reaction. The reversible potential in alkaline solution is 0.303 V (vs Hg/HgO). However in order to generate oxygen at an appreciable rate an overpotential of several hundred millivolts may be required. The net reaction takes the following form

$$O_2 + 2H_2O + 4e^- \leftrightarrows 4OH^- \quad (9)$$

Hence the process may be regarded as a proton coupled electron transfer process which occurs over a number of steps which will include both electron transfer and chemical steps, and will also involve adsorbed intermediates. The surface coverage of reaction intermediates may well vary with electrode potential. Consequently the analysis of the oxygen evolution reaction thermodynamics and kinetics is challenging. In recent years the TEECE group at Trinity College have made significant progress in the understanding of the OER. First it must be noted that the OER at oxidized metal and metal oxide electrodes involves the active participation of the oxide. Second, the acid/base behaviour of the oxide layer is an important factor : the oxide is anionic (as noted previously when discussing super-Nernstian behaviour (see fig. 12 for nickel oxy-hydroxide thin films grown on Ni metal support surfaces), and, as illustrated in fig.13 for nickel oxy-hydroxide thin films grown on nickel electrodes in aqueous base the OER onset potential decreases in a linear manner to less positive potentials with increasing solution pH which mirrors the variation of the redox switching peaks. Third, the activity of the oxide film can be ascribed to the presence of active surface or surfaquo groups which are octahedrally co-ordinated and interlinked throughout the hydrous oxide matrix. Hence the catalysis of oxidative water splitting is three dimensional. These ideas have been recently reviewed by Lyons and co-workers[24].

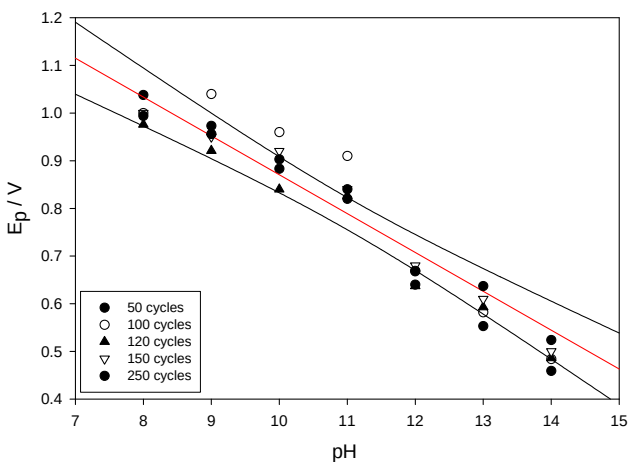

Figure 12 Variation of anodic A_2 peak potential with solution pH. Slope = - 0.082 V, r^2 = 0.96. Data measured for layers of various thickness. Nickel oxy-hydroxide layer grown via potential cycling in 1.0 M NaOH on Ni support electrodes.

The classic approach adopted to examine the kinetics of the OER at metal oxide and oxidized metal electrodes has been the use of an ensemble of steady state and transient electrochemical techniques such as Tafel Plot Polarization, Open Circuit Potential Decay (OCPD) and Electrochemical Impedance Spectroscopy[22]. These measurements yield key parameters such as the Tafel slope b and the reaction order m of the mechanistically significant reactant such as the hydroxide ion when studies are conducted in alkaline solution. The latter data are of mechanistic significance and can be used to propose a chemically meaningful step by step mechanism for the multistep OER . Electrochemical impedance spectroscopy data can be directly fitted to a proposed electrical equivalent circuit which is developed from a mathematical analysis of the proposed OER mechanistic sequence. The components of the equivalent circuit (resistors, capacitors etc) can in many cases be assigned to physically meaningful parameters and processes such as rate constants (via Faradaic impedance), film resistances, and ionic and electronic transport rates.

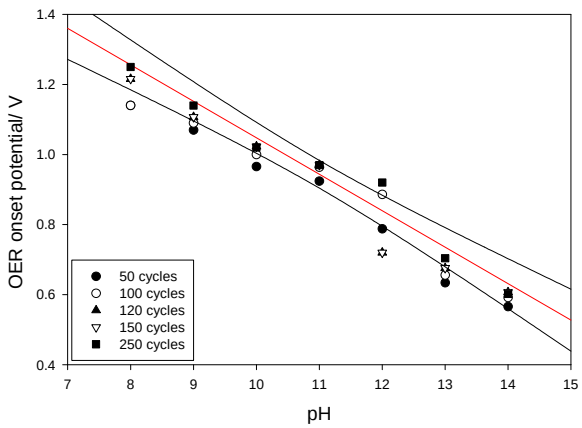

Figure 13 Variation of oxygen evolution onset potential with solution pH. Slope = - 0.104 V/dec, r^2 = 0.97. Data measured for layers of various thickness. Nickel oxy-hydroxide layer grown via potential cycling in 1.0 M NaOH on Ni support electrodes.

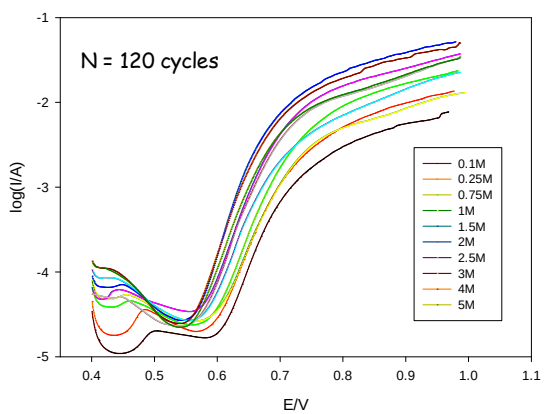

Figure 14 Typical Tafel plots for OER at multicycled nickel oxy-hydroxide thin films grown for N = 120 cycles in 1 M NaOH. Plots were recorded as function of base concentration.

Typical Tafel plots for oxygen evolution at hydrous nickel oxy-hydroxide thin films grown via potential cycling (N = 120 cycles) on Ni support electrodes are presented in fig.14. The latter data is expressed in conventional Tafel format where the OER rate is expressed as the logarithm of the current and the reaction driving force is the electrode potential. According to the Tafel equation the OER rate is exponentially dependent of the applied potential. The Tafel slope b is given by b = dE/d log i. We note dual Tafel slope behaviour with a slope of 60 mV/dec at low potentials and 120 mV/dec at higher potentials. The latter values are mechanistically significant. The reaction order is obtained by plotting the logarithm of the oxygen evolution current density recorded at a fixed electrode potential as a function of the logarithm of the hydroxide ion activity. This was done for potentials located in the low and high Tafel slope region at typical values of reaction order were $m_{OH^-} \approx 0.9$. Similar results were obtained for electro-precipitated nickel oxy-hydroxide films grown on gold support electrodes.

We have recently proposed[25] that the following set of reaction steps may be proposed to account for the mechanism of electrochemical oxygen evolution at nickel oxy-hydroxide electrodes in aqueous alkaline solution. Our mechanistic thinking is guided by the earlier work of Kobussen and Broers[26] . The mechanism is presented in schematic form in scheme B. Note that octahedrally co-ordinated oxy-nickel surfaquo groups are identified as the catalytically active species and are located within the hydrous layer. The following reaction sequence based on scheme B may be outlined:

$$SOH_2 + OH^- \rightarrow SOH^- + H_2O \quad (10)$$

$$SOH^- \rightarrow SOH + e^- \quad (11)$$

$$SOH + OH^- \rightarrow SO^- + H_2O \quad (12)$$

$$SO^- \rightarrow SO + e^- \quad (13)$$

$$SO + OH^- \rightarrow SOOH + e^- \quad (14)$$

$$SOOH + OH^- \rightarrow SO_2 + H_2O + e^- \quad (15)$$

$$SO_2 + OH^- \rightarrow SOH^- + O_2 \quad (16)$$

In the latter scheme S represents the surfaquo group which is attached to the hydrous oxide surface by bridging oxygen ligands.

The Lyons-Doyle reaction sequence[25] is presented schematically in scheme 3 The initial deprotonation step involves a bound water molecule attached to an octahedrally co-ordinated Ni(III) surfaquo group located within the hydrous layer. A common feature of these schemes is that the starting point for the OER catalytic cycle is usually represented as a metal coordinated water molecule. However, in the strongly alkaline conditions used in this system it is likely that a significant proportion of these coordinated water molecules will be deprotonated. The pK_a value for a water molecule coordinated to a highly charged metal atom is generally in the range pK_a 5-9 [27]. In light of this, it is more reasonable to assume that the initial deprotonation step expressed in eqn.10 is facile and will occur outside of the catalytic cycle.

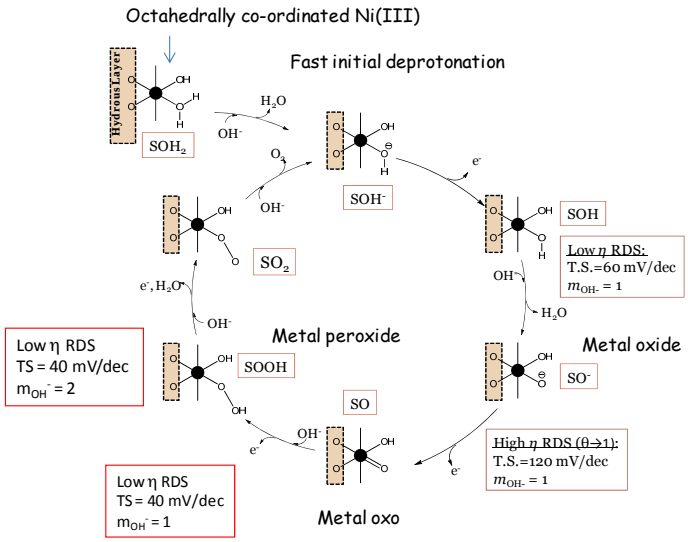

Scheme 3. Lyons Doyle reaction sequence for electrolytic generation of molecular di-oxygen at nickel oxygroups located within the hydrous oxide layer in aqueous alkaline solution.

Hence, the initial deprotonation step is depicted as a pre-step in Scheme 3 and the OER catalytic cycle begins with the resultant coordinated OH^- ion which we label SOH^-. A second point of note regarding Scheme B is that the formation of the metal oxide SO^- (eqn.12) and metal oxo SO (eqn. 13) species are designated as rate determining. Interestingly, in a recent theoretical study Muckermann *et al.* [28] showed, through the use of DFT calculations, that for a GaN/ZnO surface with high coverage of adsorbed OH^- ions the intermediate associated with the highest energy was an oxide radical. Similarly, Rossmeisl *et al.* [29] performed a DFT study of the OER at RuO_2 surfaces. They too found, for a surface saturated with adsorbed OH, that the highest energy intermediate was a surface oxygen species, in this case an oxo species. Considering these studies, the present mechanistic interpretation brings together a number of strands in the current understanding of the OER at metal oxides, and resonates with recent work proposed for water oxidation using transition metal complexes in homogeneous solution. The 60 mV/dec Tafel slope and associated reaction order of unity is associated with rate determining generation of metal oxide species (eqn.12) whereas the Tafel slope of 120 mV/dec observed for all base concentrations at high potentials and associated unity reaction order with respect to hydroxide ion activity is rationalized by assuming that the decomposition of metal oxide to form metal oxo species is slow and rate determining (eqn.13). We also note from scheme 3 that rate determining decomposition of the nickel oxo species or indeed rate determining decomposition of the nickel peroxide moiety would suggest a different set of diagnostic parameters, namely low potential Tafel slope values of ca. 40 mV/dec for both options and reaction orders wrt hydroxide ion activity of 1 and 2 for oxo decomposition (eqn.14) and peroxide decomposition (eqn.15) respectively. The catalytic cycle

illustrated in scheme 3 has been used to rationalize the OER kinetics and mechanism both at hydrous Fe and Ni oxy-hydroxide thin film modified electrodes. One of the key steps in our proposed mechanism involves the formation of a surface bound metal oxo species (SO). In scheme 3 above this species is depected as M=O suggesting a M(V) metal centre. However, this species could also be represented as a metal oxyl moiety M(IV)-O· . Indeed the degree of radical character has been shown to depend on the length of the metal oxo bond with M(V)=O being more stable for shorter bond lengths[30]. In the case of Fe the metal oxo species possibly involves Fe(V) [31] as inferred from recent variable temperature mass spectrometry data obtained for a biomimetric non-heme Fe complex with an Fe(V) oxo as the catalytic centre. The situation in the case of Ni is less clear. The Ni-O bond may be longer and have a greater radical character and a Ni(IV) oxyl intermediate may be the better descriptor of the situation.

The important point to note is that the surfaquo group structures outlined in the catalytic cycle presented in scheme 3 reflects current thinking in the allied field of water oxidation in homogeneous solution via molecular catalysts [32]. This is not unexpected given the very dispersed and somewhat tenuous nature of the catalytically active hydrous oxide layer which we postulate to be formed electrochemically on the electrode surface after cyclic polarization of the support electrode in aqueous alkaline solution.

Concluding Remarks and Future Outlook

In this paper we have presented a survey of some recent work on electrochemically prepared nickel oxy-hydroxide materials deposited as thin films on conductive gold and nickel support surfaces. The redox chemistry of the latter materials has been described in terms of electron transfer along connected surfaquo groups located within a microdispersed polymeric matrix of oxide strands immobilized on the support electrode surface. The application of these films as new generation solid state pH sensors and as efficient electrocatalysts for the electrolytic generation of molecular di-oxygen gas has been demonstrated. We have noted that the acid/base behaviour of the electrochemically prepared films is an important factor to take into account when considering the mechanism of oxygen evolution. An important new mechanism has been proposed for the OER at nickel oxide modified electrodes based on electrochemical, spectroscopic and DFT studies both in our laboratory and in others. We conclude that metal oxide and oxo species are active intermediates in the multistep OER under electrochemical conditions in aqueous solution. Indeed we can conclude that the chemistry of the surfaquo group determines the chemistry of the OER catalytic cycle.

Acknowledgements

This publication has emanated in part from research conducted with the financial support of Science Foundation Ireland (SFI) under grant number SFI/10/IN.1/I2969. The authors would like to thank Dr Michael Brandon and Prof Paula Colavita for useful discussions MEGL would like to acknowledge the late Prof. L.D. Burke for introducing him to the fascinating and important topic of metal oxide electrochemistry many years ago. For information regarding postgraduate and postdoctoral research opportunities please do not hesitate to email melyons@tcd.ie

References

1. (a) N.T. Beukes, J. Badenhorst, *J. South African Institute Mining & Metallurgy*, **2009**, 109, 343-356. (b) Z.S. Msindo, V. Sibanda, J.H. Potgieter, *J. Appl. Electrochem*., **2010**, 40, 691-699
2 (a) K. Zeng, D. Zhang, *Prog. Energy Combust. Sci*., 2010, 36, 307. (b) H. Tributsch, *Int. J. Hydrogen Energy*, 2008, 33, 5911. (c) G.W. Crabtree, M.S. Dresselhaus, M.V. Buchanan, *Phys. Today*, 2004(12) 39.
3. (a) K. Kinoshita, *Electrochemical Oxygen Technology*, Wiley Interscience, New York, 1992, Chapter 2, pp. 78-99.(b) J. Ohi, J. Mater Res., 2005, 20, 3180. (c) L.D. Burke, M.E.G. Lyons, M. McCarthy, *Adv. Hydrogen Energy*, **1982**, 3, 267.
4. D.E. Hall, *J. Electrochem. Soc*., **1983**, 130, 317-321.
5.(a) M.E.G. Lyons, S. Floquet, *Phys.Chem.Chem.Phys*., **2011**, 13, 5314-5335.(b) M.E.G. Lyons, L.D. Burke, *J. Chem. Soc. Faraday Trans. I.*, **1987**, 83, 299.
6. A. Michas, F. Andolfatto, M.E.G. Lyons, R. Durand, *Key Eng. Mat*., **1992**, 72-74, 535.
7. (a) P.W.T. Liu, S. Srinivasan, *J. Electrochem. Soc*., **1978**, 125, 1416. (b) M.E.G.Lyons, M.P. Brandon, *J. Electroanal. Chem*., **2010**, 641, 119. (c) M.E.G. Lyons, M.P. Brandon, *Phys. Chem. Chem. Phys.*, **2009**, 11, 2203. (d) M.E.G. Lyons, M.P. Brandon, *Int. J. Electrochem. Sci.*, **2008**, 3, 1463.
8. L.D. Burke, M.E.G. Lyons, *Modern Aspects Electrochemistry*, R.E. White, J.O'M. Bockris, B.E. Conway, Plenum Press, New York, **1986,** 18, 169-248.
9. (a) A.J. Terezo, J. Bisquert, E.C. Pereria, G. Garcia-Belmonte, *J. Electroanal. Chem*., **2001**, 508, 59-69. (b) J. Bisquert, G. Garcia-Belmonte, F. Fabregat Santiago, N.S. Ferriols, M. Yamashida, E.C. Periera, *Electrochem. Commun*., **2000**, 2, 601-605.
10. (a) L.D. Burke, D.P. Whelan, *J. Electroanal. Chem.*, **1980**, 109, 385. (b) A.C. Chialvo, W.E. Triaca, A.J. Arvia, *J. Electroanal. Chem*., **1983**, 146, 93.
11. (a) L.D. Burke, T.A.M. Twomey, *J. Electroanal. Chem*., **1984**, 162, 101. (b) L.D. Burke, T.A.M. Twomey, *J. Electroanal. Chem.*, **1984**, 167, 285.
12. (a) T. Ohligschlager, G. Schwitzgebel, *Phys. Chem. Chem. Phys*., **2001**, 3, 5290-5296. (b) B.S. Yeo, A.T. Bell, *J. Phys. Chem.C*., **2012**, 116, 8394-8400. (c) B.S. Yeo, A.T. Bell, *J. Am. Chem. Soc*., **2011**, 133, 5587-5593.
13. L.D. Burke, E.J. M. O'Sullivan, *J. Electroanal. Chem.*, **1981**, 117, 155.
14. (a) S.D. James, *J. Electrochem. Soc*., **1969**, 116, 1681. (b) J.W. Schultze, K.H. Vetter, *Electrochim. Acta*., **1973**, 18, 889.
15. H. Bode, K. Dehmelt, J. Witte, *Electrochim. Acta*., **1966**, 11, 1079.
16. (a) S.L. Medway, C.A. Lucas, A. Kowal, R.J. Nichols, D. Johnson, *J. Electroanal. Chem.*,**2006**, 587, 172-181. (b) M. Wehrens-Dijksma, P.H.L. Notten, *Electrochim. Acta*, **2006**, 51, 3609-3621. (c) G.T. Cheek, W.E. O'Grady, *J. Electroanal. Chem.*, **1997**, 421, 173-177. (d) H.M. French, M.J. Henderson, A. R. Hillman, E. Vieil, *J. Electroanal. Chem*., **2001**, 500, 192-207. (e) M. Gonsalves, A.R. Hillman, *J. Electroanal. Chem.*, **1998**, 454, 183-202.
17. (a) L.D. Burke, M.E.G. Lyons, E.J.M. O'Sullivan, D.P. Whelan, *J. Electroanal. Chem*., **1981**, 122, 403-407. (b) L.D. Burke, M.E.G. Lyons, D.P. Whelan, *J. Electroanal. Chem*., **1982**, 139, 131-142. (c) L.D. Burke, M.E.G. Lyons, *J. Electroanal. Chem*., **1986**, 198, 347-368.
18. M.E.G. Lyons, R.L. Doyle, M.P. Brandon, *Phys. Chem. Chem. Phys.*, **2011**,13, 21530.
19. L.D. Burke, D.P. Whelan, *J. Electroanal. Chem*., **1984**, 162, 121.

20. M.E.G. Lyons, L. Russell, M. O'Brien, R.L. Doyle, I. Godwin, M.P. Brandon, *Int. J. Electrochem. Sci.*, **2012**, 7, 2710-2763.
21. (a) S. Sunde, I.A. Lervik, L.E. Owe, M. Tsypkin, *J. Electrochem. Soc.*, **2009**, 156, B927-B937. (b) S. Sunde, I. A. Lervik, M. Tsypkin, L. E. Owe, *Electrochim. Acta*, **2010**, 55, 7751-7760. (c) F. Fabregat-Santiago, G. Garcia-Belmonte, J. Bisquert, N.S. Ferriols, P.R. Bueno, E. Longo, J. S. Anton, S. Castro-Garcia, *J. Electrochem. Soc*., **2001**, 148, E302-E309. (d) L. Sziraki, L. Bobics, *Electrochim. Acta*., **2002**, 47, 2189-2197.
22. (a) J. Bisquert, G. Garcia-Belmonte, F. Fabregat-Santiago, Noemi S. Ferriols, M. Yamashita, E. C. Pereira, *Electrochem. Commun.,* **2000**, 2, 601-605. (b) J. Bisquert, *Phys. Chem. Chem. Phys.,* **2000**, 2, 4185-4192 and references therin. (c) J. Bisquert, G. Garcia-Belmonte, F. Fabregat-Santiago, P.R. Bueno, *J. Electroanal. Chem.,* **1999**, 475, 152-163. (d) G. Garcia-Belmonte, J. Bisquert, E.C. Pereira, F. Fabregat-Santiago, *J. Electroanal. Chem.,* **2001**, 508, 48-58.
23. N. Cherchour, C. Deslouis, B. Messaoudi, A. Pailleret, *Electrochim. Acta*, **2011**, 56, 9746-9755.
24. S. Rebouillat, M.E.G. Lyons, M.P. Brandon, R.L. Doyle, *Int. J. Electrochem. Sci.*, **2011**, 6, 5830-5917.
25. (a) M.O'Brien, L. Russell, I. Godwin, R.L. Doyle, M.E.G. Lyons, , 221st ECS Meeting, Seattle, Washington, USA, May 2012, *ECS Transactions* **2012**, 45, In press. (b) R.L. Doyle, M.E.G. Lyons, 221st ECS Meeting, Seattle, Washington, USA, May 2012, *ECS Transactions* **2012**, 45, In press.
26. A.G.C. Kobussen, G.H.J. Boers, *J. Electroanal. Chem.*, **1981**, 126, 221.
27. G.A. Lawrence, *Introduction to coordination Chemistry*, p. 199, Wiley, West Sussex, 2010.
28. X. Shen, Y.A. Small, J. Wang, P.B. Allen, M.V. Fernandez-Serra, M.S. Hybertsen, J.T. Muckerman, *J. Phys. Chem.* C, **2010**, 114, 13695.
29. J. Rossmeisl, Z.W. Qu, H. Zhu, G.J. Kroes, J.K. Norskov, *J. Electroanal. Chem.*, **2007**, 607, 83.
30. (a) M. Busch, E. Ahlberg, I. Panas, *Phys. Chem. Chem. Phys*., **2011**, 13, 15062. (b) P.E.M. Siegbann, R.H. Crabtree, *J. Am. Chem. Soc*., **1999**, 121, 117.
31. A.R. McDonald, L. Que, *Nature*, 2011,3, 761.
32. (a) L.P. Wang, Q. Wu, T. Van Voorhis, *Inorg. Chem*., 2010, 49, 4543. (b) L. Duan, F. Bozoglian, S. Mandal, B. Stewart, T. Privalov, A. Llobet, L. Sun, *Nature*, 2012, 4, 418.

Mike Lyons is currently Professor in Physical Chemistry and SFI Principal Investigator in the School of Chemistry & CRANN, Trinity College Dublin, Ireland. He was born in Cork city in 1956 and is a graduate of University College Cork (1979) where he read Chemistry and Mathematical Physics and obtained his Ph.D degree from the same University in 1983 under the supervision of Prof. Declan Burke in metal oxide electrochemistry. He worked with Prof. John Albery and Prof. Brian Steele at Imperial College London on metal oxide electrocatalysis before being appointed to a lectureship in Physical Chemistry at Trinity College Dublin in 1984. He was elected to Fellowship, Trinity College Dublin, in 1992 on the basis of publication and research. Mike has served both on the University Academic Council and Governing Body (Board) of Trinity College, and has been Director of Undergraduate Teaching & Learning and Head of Physical, Computational and Materials Chemistry within the School of Chemistry. His research interests encompass Physical and Analytical Electrochemistry and in a publication output of two books and more than 100 papers, he has made significant contributions to electrode kinetics, metal oxide electro-catalysis, electroactive polymer electrochemistry, mathematical modelling of electrochemical systems, electrochemical biosensors, and carbon nanotube electrochemistry. His H-index is 25. His current interests in collaboration with the recently formed SFI funded Trinity Electrochemical Energy Conversion and Electrocatalysis Group, is in revisiting and finally understanding the redox and electrocatalytic behaviour with respect to oxygen evolution, oxygen reduction and hydrogen evolution of hydrous oxide coated metal and metal oxide electrodes for use in energy conversion and storage device applications. His group is also developing non enzymatic electrochemical biosensors based on metal oxide modified electrodes for bio-diagnostic applications and examining the use of metal oxide electrodes as new generation pH sensors.